# Research on Wave Characteristics of Large-scale Lakes Based on the Mild-slope Model

Yanxia Zhang[1], Kai Wang[1,*], Han Sun[1], Xixi Wang[1], Junyu Zheng[1], and Yichen Huang[2]

[1]Jiangsu Survey and Design Institute of Water Resources Co, Ltd., Yangzhou, Jiangsu Province 225100, China
[2]Hohai Univerisity, Nanjin, Jiangsu Province, 210000, China

*Corresponding author's e-mail:wankae@qq.com

**Abstract.** Lakes, as invaluable natural resources, serve multifaceted roles encompassing flood prevention, water supply, and ecological balance. However,Wind-induced waves within lake regions exert a pronounced influence on shoreline development and the proliferation of aquatic vegetation. Wind-induced waves seriously affects the safety of levee projects and the benefit of lakes. This study delves into wind-wave dynamics in lakes using the mathematical model—the mild-slope equation. It aims to unveil the characteristics and distribution of wind and wave patterns across manifold embankment sections under diverse water levels and wind directions. These findings are instrumental in refining shoreline designs, selecting appropriate aquatic flora, and providing robust data support for constructing flood control systems and managing the ecological environment along lake perimeters.

**Keywords:** Hongze Lake; Waves; Wind speed; Characteristics; Mild-slope model.

## 1 Introduction

Lakes embrace a multitude of functions and benefits, functioning as pivotal natural resources and strategic economic resources [1]. Jiangsu Province is among the regions in China where freshwater lakes are notably concentrated, racking up a cumulative area of 6260 square kilometers and a combined storage capacity equivalent to 13.11 billion cubic meters. The lake-to-land ratio in this province yields 6%, leading the nation in terms of lake coverage. These lakes, as exceptional natural assets, play a crucial role in various aspects, including flood control, water supply, navigation, tourism, aquaculture, biodiversity preservation, and water purification [2]. Their contributions significantly safeguard the local economic and social development.

The lakes harbor abundant aquatic resources and have historically been revered for their rich fish, shrimp, crab, and shellfish reserves, often acclaimed as sites for raking in the dough. However, driven by economic interests, agricultural development, urban


P. Xiang et al. (eds.), *Proceedings of the 2023 5th International Conference on Hydraulic, Civil and Construction Engineering (HCCE 2023)*, Atlantis Highlights in Engineering 26,
https://doi.org/10.2991/978-94-6463-398-6_4

construction along the lakes, and aquaculture practices have led to a worsening shrinkage of the lakes. This trend is accompanied by unregulated exploitation of resources such as lakeshores, water bodies, biota, and landscapes, resulting in a severe decline in their functions related to flood control, ecological balance, and scenic beauty. In recent years, Jiangsu Province has significantly doubled efforts to protect the ecological balance of its lakes. Initiatives such as "returning polders to lakes" and "returning fishing zones to wetlands" have been implemented, effectively restoring the lake surface area. Additionally, flood prevention and ecological restoration projects have been enacted, reinforcing flood embankments and conducting ecological restoration activities. These efforts aim not only to enhance regional flood control capabilities but also to further restore lake capacity and improve the overall ecological environment of the lakes.

Wind-induced waves represent a highly variable environmental factor that exerts profound and intricate influences on the construction of flood embankments around lakes and the ecosystem [3]. Therefore, this study investigates the characteristics of wind-induced waves in lake regions to comprehend the distribution of waves across various lake sections. The findings contribute valuable data support for establishing flood prevention systems within lakes and governing the ecological environment along their shores. Ultimately, this endeavor ensures the secure and sustainable development of the region.

### 1.1 Basic information on the lake

Hongze Lake stands as the fourth-largest freshwater lake in China and is the foremost lake within the Huai River Basin. It serves as a crucial reservoir for the South-to-North Water Diversion Project and holds multifaceted functions encompassing flood control, water supply, ecology, cultural significance, navigation, and fisheries. Spanning 65 kilometers in length with an average width of 24.4 kilometers, the lake covers an area of 2,069 square kilometers, reaches a maximum depth of 5.5 meters, and has a flood control capacity of 13.5 billion cubic meters. Characterized as a large, shallow lake, Hongze Lake exhibits a shallow saucer-shaped basin, gentle sloping shorelines, a gradual incline from the shores towards the center, and a relatively flat lakebed, typically situated between elevations of 10 to 11 meters [4]. Hongze Lake demonstrates distinct features such as extensive fetch, limited shoreline vegetation during winter-spring seasons, and a high storage level. Concurrently, efforts involving actions on "returning polders to lakes" and "reinforcing embankments to mitigate flooding" are ongoing. However, these initiatives introduce challenges regarding embankment safety due to direct exposure to wind-induced waves within lakes. Additionally, the initiative of "returning polders to lakes" might lead to difficulties in sustaining aquatic plant life and subsequent degradation of the aquatic ecosystem, causing a reduction in biodiversity. Addressing these issues requires prudent management. Against this backdrop, it becomes crucial to study the wind-induced wave characteristics using Hongze Lake as a case study, given its typicality and immediate relevance.

### 1.2 Research content and scenarios

Drawing upon wind speed data obtained from engineering water bodies and their surrounding areas, we estimate the design wind speeds for different directions and time periods within the lake region. We then proceed to select an optimal mathematical model for simulating waves, conducting computations using this chosen wave model. This involves integrating the topography of the lake region with meteorological data to perform mathematical model experiments under various combinations of directions and water levels. The outcome of these experiments furnishes information on the distribution of waves across different parts of the lake. These findings serve as crucial data support for the construction of embankments facing the lake and for ecological restoration efforts in various sections [5-6].

Hongze Lake presents characteristic water levels: the dead water level at 11.3 m, the flood-limited level at 12.5 m, the normal storage level during non-flood periods at 13.5 m, the activation level for the flood detention zone at 14.5 m, and the design flood level at 16.0 m. Based on these characteristic water levels and engineering functionalities [7], the following research scenarios are proposed: (1) During periods of flood retention in the surrounding flood detention zones with an activated level of 14.5 m [8], corresponding to the encounter of significant inflows during flood seasons, the research scenario will consider the design wind speeds for the flood season; (2) When the lake operates at the normal storage level of 13.5 meters and encounters water diversions from the East Route of the South-to-North Water Diversion Project [9], the research scenario will correspond to design wind speeds during winter-spring seasons.

## 2 Wind speeds around the Lake

### 2.1 Overview of regional wind speeds

The Xuyi Meteorological Station and Sihong Meteorological Station are situated in the vicinity of Hongze Lake. A robust correlation emerges in the wake of comparing the wind rose diagrams and correlating wind speeds of the two stations. Both Xuyi and Sihong Meteorological Stations exhibit a strong correlation in wind direction and speed, boasting a noteworthy correlation coefficient (R) of 0.81. Notably, the Xuyi Meteorological Station, positioned at a relatively elevated location and closer to the lake, experiences minimal influence from surface factors. Consequently, the measured wind speeds at Xuyi slightly surpass those recorded at Sihong Meteorological Station. As a safety measure, the wind speed data from the Xuyi Meteorological Station is utilized in the calculation of design wind speeds [10]. At the Xuyi Meteorological Station, the prevailing wind direction aligns with east-southeast to east (ESE), occurring with a frequency of occurrence at 12.1%, closely followed by east (E) at 11.5%. Both directions demonstrate roughly equivalent frequencies, notably higher than those of other wind directions. Wind rose diagram as follows Figure 1, Figure 2.

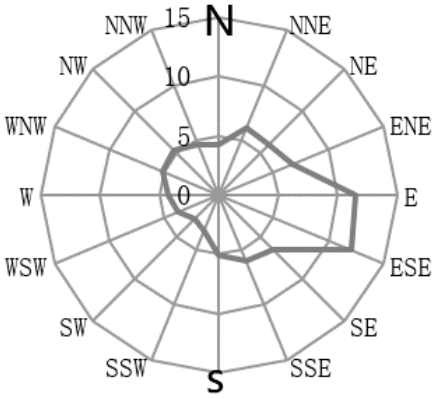


**Fig. 1.** Wind rose diagram of Xuyi Meteorological Station (2012 to 2019)

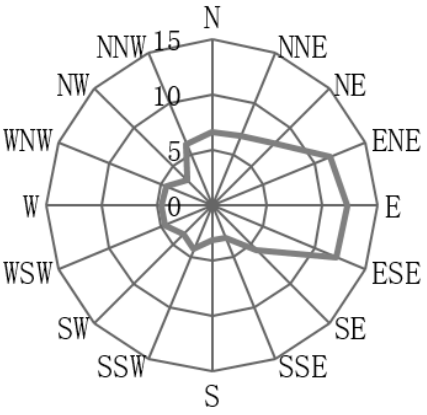


**Fig. 2.** Wind rose diagram of Sihong Meteorological Station in 2020

## 2.2 Research on design wind speeds

The wind speed data from the Xuyi Meteorological Station, being land-based, requires adjustments for both height and land-water discrepancies to match the wind speed at a height of 10 meters above the water surface, utilizing data from 10-minute average wind speeds. Height adjustment and land-water corrections [11-12]for wind speed follow methods recommended in the *Design of Dam Wave Protection and Slope Protection* and the *Hydrological Code for Ports and Waterways*. The maximum wind speeds (10-minute average) from different directions during the flood season and winter-spring seasons over 30 years (1991 to 2020) at the Xuyi Meteorological Station were adjusted to the 10-meter height above the lake surface and multiplied by a factor of 1.5. This process ultimately yields the design wind speeds for the flood season and winter-spring seasons in the Hongze Lake area, as illustrated in Table 1 and Table 2.

**Table 1.** Design wind speed during the flood season in the Hongze Lake area

| Direc-tion | N~NNE | NE~ENE | E~ESE | SE~SSE | S~SSW | SW~WSW | W~WNW | NW~NNW |
|---|---|---|---|---|---|---|---|---|
| Wind speed m/s | 21.6 | 18.6 | 20.2 | 19.4 | 20.4 | 18.1 | 20.6 | 21.1 |

**Table 2.** Design wind speed during winter-spring seasons in the Hongze Lake area

| Direction | N~NNE | NE~ENE | E~ESE | SE~SSE | S~SSW | SW~WSW | W~WNW | NW~NNW |
|---|---|---|---|---|---|---|---|---|
| Wind speed m/s | 23.5 | 19.7 | 21.5 | 19.0 | 19.6 | 18.9 | 21.2 | 22.2 |

It has come to light from the two tables that during the flood season, the highest design wind speed in the lake area occurs in the North to North-Northeast (N~NNE) direction, reaching 21.6 meters per second (m/s), followed by the Northwest to North-Northwest (NW~NNW) direction at 21.1 m/s. Winds from the West to West-Northwest (W~ENW) direction have a speed of 20.6 m/s, slightly lower than those from the Northwest to North-Northwest (NW~NNW). The lowest design wind speed among these directions is in the Southwest to West-Southwest (SW~WSW) direction, measuring 18.1 m/s. In contrast, in winter-spring seasons, the design wind speed in the North to North-Northeast (N~NNE) direction is slightly higher at 23.5 m/s compared to that in the flood season. The Northwest to North-Northwest (NW~NNW) direction has a design wind speed of 22.2 m/s, slightly higher than during the flood season. However, in the Southeast to South-Southeast (SE~SSE) and South to South-Southwest (S~SSW) directions, the design wind speeds are 19.0 m/s and 19.6 m/s, respectively, slightly lower than their counterparts in the flood season.

### 2.3 Wind speed division and representative research sections

The wind-induced wave characteristics are primarily contingent upon the design wind speed, wind zone length, and water depth within the area. Based on varying wind directions facing the embankment in the lake area and the width of the water body in front of the embankment, wave elements are computed in segmented sections of the embankment [13]. The guiding principle for embankment segmentation lies in maintaining similar orientations of the embankment and consistent wind zone lengths and water depths along the embankment front. The following diagrams illustrate the schematic positioning for wave calculation segments under current operational conditions (Figure 3) and under conditions when the embanked area is restored to a lake (Figure 4).

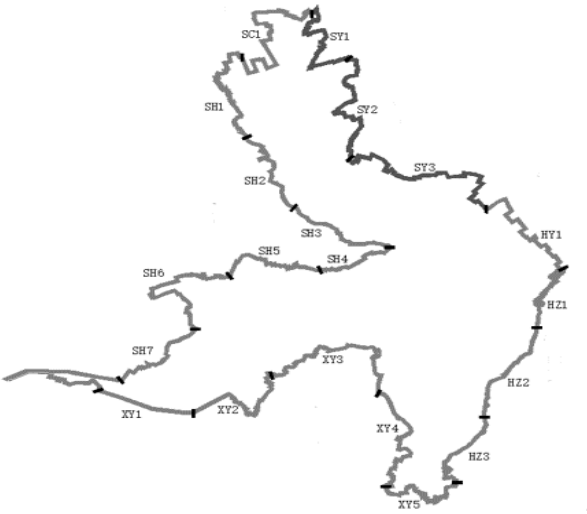


**Fig. 3.** Schematic positioning for wave calculation segments under current operational conditions


**Fig. 4.** Schematic positioning for wave calculation segments under conditions of returning polders to lakes

## 3 Mathematical model of waves

Different mathematical models for waves have their own characteristics and applicable ranges. Considering the topography of the lake area, meteorological data, and the application scenarios of these models, we conducted trial calculations using the mathematical model of the mild-slope equation, the mathematical model of the parabolic equation, and simulations of irregular waves. Finally, we opted for the mathematical model of the mild-slope equation, which comprehensively considers the effects of wave refraction, diffraction, reflection, and bottom friction [14].

Due to various factors, ocean waves undergo multitudinous complex changes upon entering shallow coastal areas. Changes in the terrain lead to phenomena such as refraction and deformation in shallow waters. When encountering obstacles like islands or breakwaters, waves can circumvent these barriers, propagating into sheltered areas behind them, causing wave diffraction. Along steep coastlines, breakwaters, docks, and protective structures, waves propagating forward can be reflected back, and the steep underwater terrain also significantly influences the incoming wave reflections. In order to capture these phenomena, it is essential to establish comprehensive mathematical models that factor in refraction, diffraction, and reflection of waves. The mathematical model of the mild-slope equation successfully integrates refraction and diffraction models. It converts to the refraction equation when neglecting diffraction effects, transforms into the diffraction equation when water depth remains constant, and aligns with the shallow-water long wave equation in very shallow waters. Therefore, this model is applicable for the combined calculation of wave refraction, diffraction, and reflection under various water depths with small-amplitude waves [15-17].

The extended form of the mild-slope equation considering wave energy dissipation and wind energy input is presented as follows:

Steady state:

$$\nabla_h \cdot \left( CC_g \nabla_h \Phi \right) + \left( k^2 CC_g + i\omega F \right) \Phi = 0 \tag{1}$$

Unsteady state:

$$\frac{\partial^2}{\partial t^2} \Phi - \nabla_h \cdot \left( CC_g \nabla_h \Phi \right) + \left( \omega^2 - k^2 CC_g - i\omega F \right) \Phi = 0 \tag{2}$$

where $C$ and $C_g$ represent wave velocity and wave group velocity, $\Phi$ denotes wave potential, $k$ is the number of waves, $\omega$ stands for the angular frequency, $F$ signifies the variation factor of wave energy, and $i = \sqrt{-1}$.

Using the Alternating Direction Implicit (ADI) method with a relaxation factor, the discrete equation divides a time step $\Delta t$ into two steps. The resulting difference scheme is as follows:

$$f_{i,j}\frac{\phi_{i,j}^{n+1/2}-\phi_{i,j}^{n}}{\frac{1}{2}\Delta t}=\delta_x^2\phi_{i,j}^{n+1/2}+\frac{1}{2}\left(k_c^2\right)_{i,j}\phi_{i,j}^{n+1/2}+\delta_y^2\phi_{i,j}^{n}+\frac{1}{2}\left(k_c^2\right)_{i,j}\phi_{i,j}^{n} \tag{3}$$

$$f_{i,j}\frac{\phi_{i,j}^{n+1}-\phi_{i,j}^{n+1/2}}{\frac{1}{2}\Delta t}=\delta_x^2\phi_{i,j}^{n+1/2}+\frac{1}{2}\left(k_c^2\right)_{i,j}\phi_{i,j}^{n+1/2}+\delta_y^2\phi_{i,j}^{n+1}+\frac{1}{2}\left(k_c^2\right)_{i,j}\phi_{i,j}^{n+1} \tag{4}$$

$$\phi_{i,j}^{n+1}=\lambda\widetilde{\phi}_{i,j}^{n+1}+(1-\lambda)\phi_{i,j}^{n} \tag{5}$$

There are two types of boundary conditions:

(1) Incident wave boundary condition:

$$\frac{\partial\phi}{\partial n}=ik\left(\phi_i-\phi_r\right)=2ik\phi_i-ik\phi \tag{6}$$

where $\phi_i$ denotes the incident wave potential, $\phi_r$ means the reflected wave potential, and $n$ refers to the incident wave direction.

(2) Transmission and reflection boundary condition.

$$\frac{\partial\phi}{\partial n}-ik\gamma\cos\alpha\phi=0 \tag{7}$$

where α represents the angle between the wave direction and the boundary normal, $\gamma$ is the reflection parameter calculated by the following equation:

$$\gamma=\gamma_1+i\gamma_2 \tag{8}$$

$$\gamma_1=k\cos(\theta-\alpha)\frac{2R\sin\delta}{1+R^2+2R\cos\delta} \tag{9}$$

$$\gamma_2=k\cos(\theta-\alpha)\frac{R^2-1}{1+R^2+2R\cos\delta} \tag{10}$$

where R denotes the amplitude attenuation factor (reflection coefficient), and δ stands for phase difference. When $\gamma=0$, it signifies a total reflection boundary, whereas it denotes a total transmission boundary when $\gamma=1$.

The abovementioned method is suitable for the combined calculation of wave refraction, diffraction, and reflection, witnessing applications in various engineering projects [17-20].

# 4 Analysis result

## 4.1 Design wave elements for segments

The model calculations have yielded the wave distribution across different areas of Hongze Lake under varying directions, water levels, existing conditions, and conditions of returning polders to lakes. This paper explicitly presents the wave characteristics of the least favorable representative section at a water level of 14.5 meters under the significant wave height for each county or district. Table 3 demonstrates the wave characteristics under the existing condition. Table 4 displays the wave characteristics under the condition of returning polders to lakes. A detailed comparison of the design wave characteristics between these two conditions at the 14.5-meter water level can be visualized in Figure 5.

**Table 3.** Statistical summary of design wave elements for segments under the existing condition

| Segment position | | Design water level for flood detention in flood dike: 14.5 m | | | | | | | |
|---|---|---|---|---|---|---|---|---|---|
| | | $H_{1\%}$ (m) | $H_{4\%}$ (m) | $H_{5\%}$ (m) | $H_{13\%}$ (m) | $\overline{H}$ (m) | $\overline{T}$ (s) | L (m) | Wave direction |
| Sucheng District | SC1 | 1.46 | 1.26 | 1.22 | 1.04 | 0.68 | 3.7 | 18.6 | SSE |
| Siyang County | SY3 | 1.77 | 1.55 | 1.51 | 1.30 | 0.87 | 4.1 | 21.0 | S |
| Huaiyin District | HY1 | 1.77 | 1.54 | 1.50 | 1.30 | 0.87 | 4.1 | 20.8 | W |
| Hongze District | HZ3 | 2.15 | 1.89 | 1.84 | 1.60 | 1.09 | 4.5 | 24.7 | N |
| Xuyi County | XY5 | 1.80* | 1.77 | 1.73 | 1.53 | 1.08 | 4.4 | 21.6 | N |
| Sihong County | SH6 | 1.81 | 1.59 | 1.55 | 1.35 | 0.92 | 4.2 | 20.8 | ESE |

**Table 4.** Statistical summary of design wave elements for segments under the condition of returning polders to lakes

| Segment position | | Design water level for flood detention in flood dike: 14.5 m | | | | | | | |
|---|---|---|---|---|---|---|---|---|---|
| | | $H_{1\%}$ (m) | $H_{4\%}$ (m) | $H_{5\%}$ (m) | $H_{13\%}$ (m) | $\overline{H}$ (m) | $\overline{T}$ (s) | L (m) | Wave direction |
| Sucheng District | SC1 | 1.50* | 1.38 | 1.34 | 1.18 | 0.82 | 3.9 | 17.2 | S |
| Siyang County | SY3 | 1.81 | 1.60 | 1.56 | 1.36 | 0.93 | 4.2 | 20.6 | S |
| Huaiyin District | HY1 | 1.74* | 1.54 | 1.51 | 1.32 | 0.91 | 4.1 | 19.5 | W |
| Hongze District | HZ2 | 2.19 | 1.91 | 1.86 | 1.61 | 1.08 | 4.6 | 25.9 | NNW |
| Xuyi County | XY7 | 1.80* | 1.78 | 1.74 | 1.54 | 1.09 | 4.5 | 21.7 | N |
| Sihong County | SH6 | 1.80* | 1.69 | 1.65 | 1.45 | 1.01 | 4.3 | 20.9 | ESE |

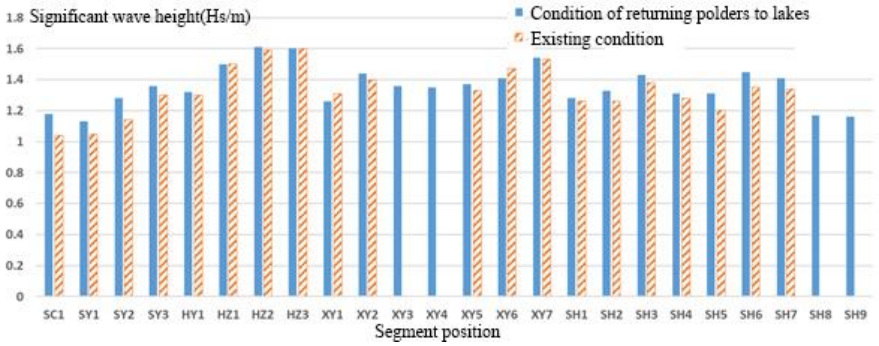


**Fig. 5.** Comparison of design wave elements for segments under the existing condition and condition of returning polders to lakes (at a water level of 14.5 m)

## 4.2 Contour maps of significant wave height

Based on the results of wave elements calculated using the mathematical model, contour maps of significant wave heights ($H_{13\%}$) for different directions in the engineering water area at 14.5 m and 13.5 m water levels are generated. This paper displays the wave element results under the existing condition and the condition of returning polders to lakes at the 14.5 m water level. The contour maps of significant wave heights ($H_{13\%}$) for the North and West directions in various segments are presented. Under different circumstances,distribution of significant wave heights as follows Figure 6,Figure 7, Figure 8, Figure 9.

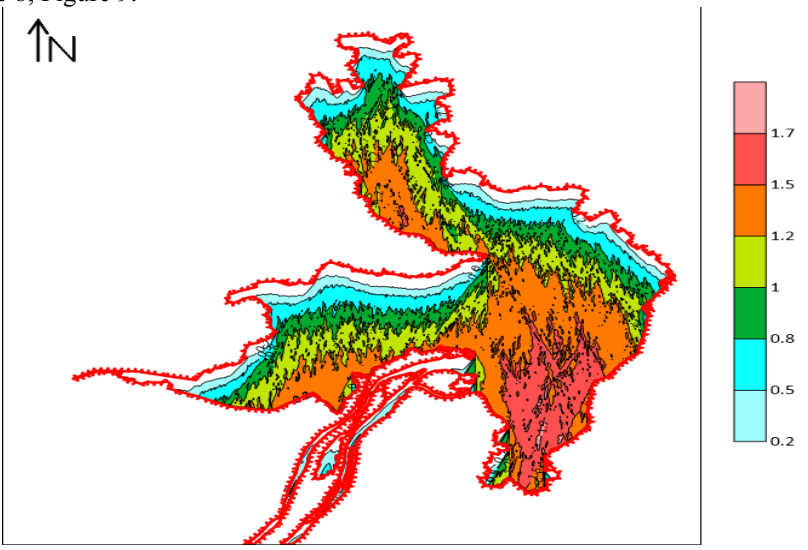


**Fig. 6.** Distribution of significant wave heights (H13%) in the N direction for engineering waters under the existing condition (14.5 m water level)

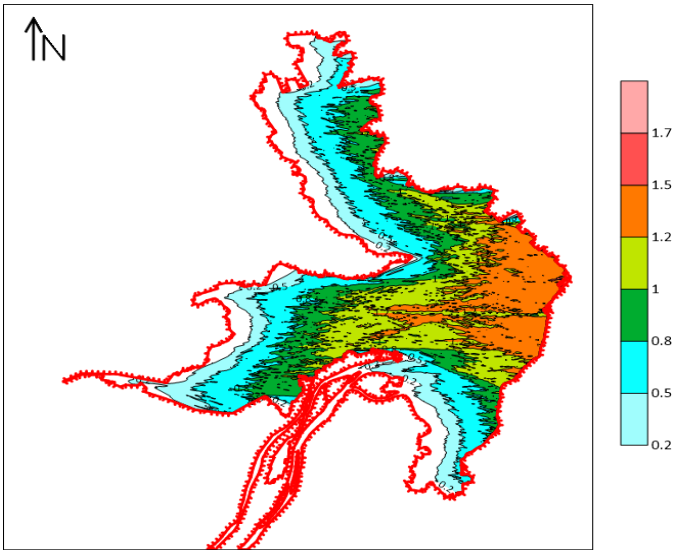


**Fig. 7.** Distribution of significant wave heights ($H_{13\%}$) in the W direction for engineering waters under the existing condition (14.5 m water level)

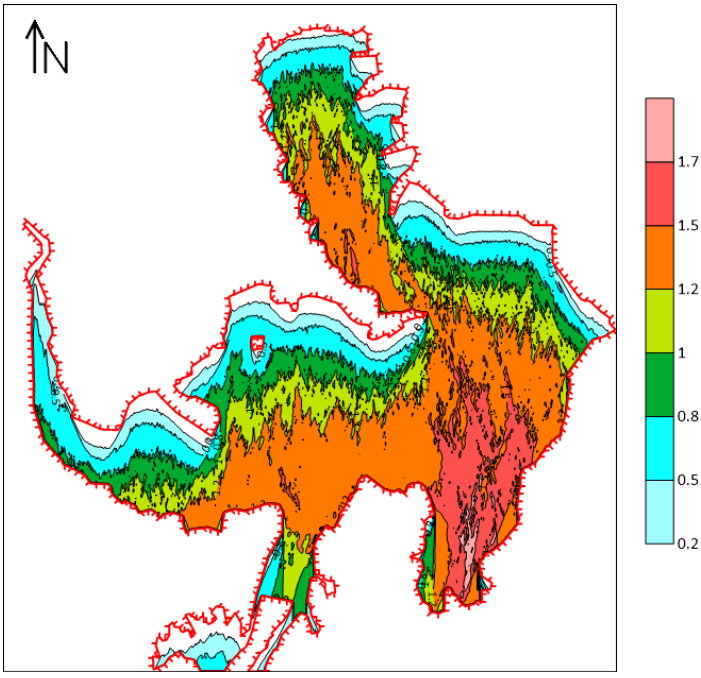


**Fig. 8.** Distribution of significant wave heights (H13%) in the N direction for engineering waters under the condition of returning polders to lakes (14.5 m water level)

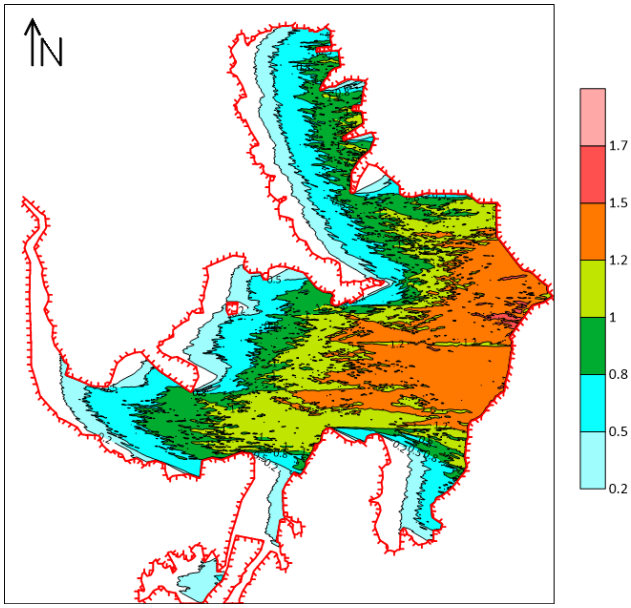


**Fig. 9.** Distribution of significant wave heights ($H_{13\%}$) in the W direction for engineering waters under the condition of returning polders to lakes (14.5 m water level)

## 5 Conclusion

Based on model calculations, when the activation water level for flood detention in Hongze Lake reaches 14.5 m, the significant wave heights in the lake area range from 1.0 to 1.6 m. During non-flood seasons, particularly when the South-North Water Diversion Project maintains the storage level at 13.5 m, the significant wave heights in the lake area range from 0.6 to 1.5 m. The highest wave heights tend to occur under the impact of winds from the N to NNW directions, notably in the Hongze District. Despite the impact of land reclamation, which extends the wind zone and reduces shoreline protection, the effect on the highest waves remains minimal. However, there are specific segments where the direction of wave action might shift [20], resulting in an escalation in wave height by approximately 0.2 m. Due to the lack of effective protection measures, the revetment in some sections of Hongze Lake will be directly hit by wind and waves after the promotion and implementation of the revetment project, and local protection should be optimized.

These findings regarding wave elements indicate varying hydrodynamic effects across different lake sections due to wind and wave interactions. This information can be leveraged to optimize the design of bank protection structures and select suitable aquatic flora capable of withstanding diverse wave-induced stresses. Such efforts aim to bolster the protective capacities of the lake area and refine the ecological composition along its shoreline [5]. The vertical distribution characteristics of wind waves can be used to guide the design of lake beach elevation design, guide the protection range of

levee feet and the selection of vegetation height, and the horizontal distribution characteristics of wind waves can be used to guide the design of beach width and vegetation density.Building upon these findings, physical model experiments on representative embankment sections can be conducted to devise suitable bank protection structures and curate a catalog of aquatic plants conducive to lake construction [21-23].

## Acknowledgment

Jiangsu Province Water Conservancy Science and Technology Project: Study on the Relationship between the Subsequent Phases of the Eastern Route of the South-to-North Water Diversion and Water Security in Northern Jiangsu (Project No.: 2021001).

## References

1. Ma R H,Yang G S,Duan H T, et al. Number, area and spatial distribution of lakes in China[J]. Science in China: Earth Sciences, 2011, 41(03): 394-401.
2. Yang G S, Ma R H, Zhang L, et al. Current status of Chinese lakes, major problems and protection strategies[J]. Lake Science, 2010, 22(06): 799-810.
3. Liang Y, Yin J X, Zhu X P, et al. Application of MIKE21 hydrodynamic model in water level simulation of Hongze Lake [J]. Hydroelectric Energy Science, 2013, 31(01): 135-137, 99.
4. Yang D Y and Wang Y F. Changes of geographic environment and floods in the Huaihe River Basin in the last 2000 years--Floods in the middle reaches of the Huaihe River and changes in Hongze Lake[J]. Lakes Science,1995, (01): 3-4, 3-7.
5. Xu H M, Zhang Z L, Wang D T, et al. Research on wind and wave characteristics and protection design of Shishu Lake in Nanjing[J]. Jiangsu Water Conservancy, 2018, (07): 1-6.
6. Ju C F. Problems and countermeasures of wind and wave resistance of ships in Hongze Lake[J]. Transportation Enterprise Management, 2015, 30(01): 33-35.
7. Chu E G. A preliminary study on the hydrological characteristics of Hongze Lake[J]. Hydrology, 2001, (05): 56-59.
8. Wang X D. Analysis of the flood control system in Huaihe River Basin[J]. China Water Resources, 2003, (19): 29-31.
9. Zhou J L. Negotiations on the layout of the planning of the South-to-North Water Diversion Project[J]. Jiangsu Water Conservancy, 2002, (01): 4-6, 11.
10. Li D L, Zhang X Q, Jin Y Q, et al. Wind and noise reduction and microclimate effects of different plant slope protection modes in the Huai'an section of the Beijing-Hangzhou Canal[J]. Journal of Ecology and Rural Environment, 2012, 28(03): 249-254.
11. Liao Z G, Zhang H, and Chen H B. Discussion on the value of wind speed for the design of ultra-high voltage transmission lines[J]. Electric Power Construction, 2006, (04): 28-32.
12. Pang J B. Observational analysis and wind tunnel simulation of strong wind characteristics in coastal and mountainous areas [D]. Tongji University, 2006.
13. Jiang Y, Luo Y, and Zhao Z C. Characteristics of wind direction changes in China in the past 50 years[J]. Journal of Applied Meteorology, 2008, 19(06): 666-672.
14. Zhou B Z. Establishment of a fully nonlinear numerical wave model in open water and its application to the platform Ringing phenomenon [D]. Dalian University of Technology, 2013.

15. Zhang D W. Mathematical modeling of dam failure flow and its application [D]. Tsinghua University, 2008.
16. Li M G, Wang Z L, and Jiang D C. Research and progress of mathematical modeling of nearshore wave propagation deformation[J]. Ocean Engineering, 2002, (04): 43-57.
17. Gu H B, Sun J S, Zheng B Y, et al. Development of mathematical modeling of nearshore waves[J]. Waterways and Harbors, 2004, (02): 78-83.
18. Wu Y S, Lian J J, Wang Z Y, et al. Modeling of wave-current interaction[J]. Journal of Water Resources, 2002, (04): 13-17.
19. Hong G W, Feng W B, and Zhang H S. Numerical simulation of wave propagation in coastal estuarine waters[J]. Journal of Hohai University (Natural Science Edition), 1999, (02): 4-12.
20. Li M G and Liu B Q. Mathematical modeling of waves in Oujiangkou sea area[J]. Waterway and Harbor, 2001, (01): 1-8.
21. Nils Goseberg. Overland flow of broken solitary waves over a two-dimensional coastal plane[J]. Coastal Engineering, 2022.
22. A.. On the synthetic aperture radar imaging of ocean surface waves[J]. Ieee Journal of Oceanic Engineering, 2003, 7(2): 96-103.
23. Stefan G. J. Aarninkhof. Longshore sediment transport by large-scale lake circulations at low-energy, non-tidal beaches: A field and model study[J]. Coastal Engineering, 2023, 180: 104268.